Inner Pressure Testing of Full-Scale Pipe Samples

R.I. Dmytriienko, S.M. Prokopchuk and O.L. Paliienko

Abstract This chapter describes the experimental tests performed with the aim of studying the reinforcement effects of a given repair system using composite material wraps intended for a damaged transmission pipeline (for petroleum, liquid petroleum products or natural gas), with defects of the metal loss type (also named volumetric surface defects). These tests have been defined based on the considerations presented in Chapter "Development of an Experimental Programme for Industrial Approbation", which details the material selection, the testing conditions and the objectives of our experiments. The sequence of the comparative hydraulic inner pressure tests, performed on full-scale samples, is detailed below. Our experiments were aimed on simulation of a pipeline under the following four conditions: as-delivered, damaged, repaired using a composite material wrap and reinforced on its entire length with composite materials. All samples have been loaded up to fracture. The properties of material used for the pipe manufacturing and the main results of hydraulic tests are also present. Based on the experimental results, presented in this chapter, an efficiency assessment (including numerical simulations using finite element method) of the investigated composite repair system has been also performed and it will be presented in Chapter "Effectiveness Assessment of Composite Repair Systems".

Keywords Hydraulic tests · Inner pressure · Pipe · Wrap

1 Preparation of Samples

Four full-scale samples, simulating the pipeline in as-delivered condition as well as in the conditions damaged, repaired and reinforced with composite wraps, were subjected to the comparative static hydraulic inner pressure tests. The reference designations of the samples are I1, I2, I3, I4, respectively. The samples were made

R.I. Dmytriienko (✉) · S.M. Prokopchuk · O.L. Paliienko
E.O. Paton Electric Welding Institute, Kiev, Ukraine
e-mail: dri1@ukr.net

E.N. Barkanov et al. (eds.), *Non-destructive Testing and Repair of Pipelines*,
Engineering Materials, DOI 10.1007/978-3-319-56579-8_26

from hollow billets, cut out from one seamless hot-worked pipe 219x6 (steel 20 [1]), produced in accordance with [2, 3 i.1.2B] at OJSC „Interpipe NTZ", Dnepropetrovsk, Ukraine. The pipe was produced with standardization of its mechanical properties and composition. All samples were equipped with flat steel bottoms of 32 mm thickness. They were manually welded-up to the hollow billets, at the edges of which a technological bevel was preliminary done. Geometry of the bottom and weld provided for the fracture of each of the samples to occur in its middle part. The bottoms were used for samples sealing.

Samples I2 and I3 included milled similar defects (see Fig. 1), simulating erosion–corrosion damage with the depth equal to 60% of the pipe thickness. Geometry of the defects was defined as described in Chapter "Development of an Experimental Programme for Industrial Approbation". The defect shapes were provided for uniform plastic deformation in the defect middle zone that simplified measurements. The relative parameters of the sample I2 defect, according to [4], are the following: depth: $\lambda_c = \frac{S_o - t_o}{S_o} = 0.60$, length: $\lambda_a = 1.258 \frac{a}{\sqrt{D_H S_o}} = 4.34$, width $\lambda_b = 1.258 \frac{b}{\sqrt{D_H S_o}} = 3.33$. These parameters are smaller by about 1.75% for the defect in sample I3.

The composite wraps were installed on samples I3 and I4 employing machine winding of direct roving ES 10 1680N-U10(168). It consists of elementary fiberglass filaments "E" [5], being wetted in hot curing epoxy binder KDA-KhI [6]. Winding was carried out on the rotating hollow billets with welded-up bottoms fixed in a special device of turning machine. The wraps were formed layer-by-layer: roving was fed through a machine support, which was moved along the sample axis with fixed step. Laying of roving was carried out under ≈90° angle to pipe axis. The average value of roving tension force for samples I3, I4 was 45 and 41N, respectively, and its oscillation due to axis misalignment of outer surface of hollow billet and machine axis ±6N. After laying the necessary amount of layers, the wraps were subjected to polymerization at 120–150 °C temperature. Actual thickness of wraps was determined after their polymerization by means of measurement of the wrap and pipe parameters. On sample I3 the wrap was installed with overlapping of the defect in axial direction. A cone transfer to pipe metal was formed at one side. On sample I4 winding covered all cylindrical surface including tack welds. Before wrap setting on sample I3 the defect cavity was filled with a compound (sections of roving of ∼15 mm length), mixed with epoxy binder of cold curing [7] for uniform transfer of force from defect surface to inner wrap surface.

Tension diagrams were obtained for the calculation of necessary amount of the w rap layers (see below) and mechanical properties of pipe material, composite material and roving were determined, samples perimeters were measured. The wrap set on sample I3 should provide for elastic behavior of metal in the defect up to test pressure as well as strength no worse than in as-delivered pipe (sample I1).

Determination of strengthening effect of the wrap depending on number of layers was carried out from the condition of mutual deformation of pipe and wrap. Description of mutual work of pipe and wrap up to fracture based on

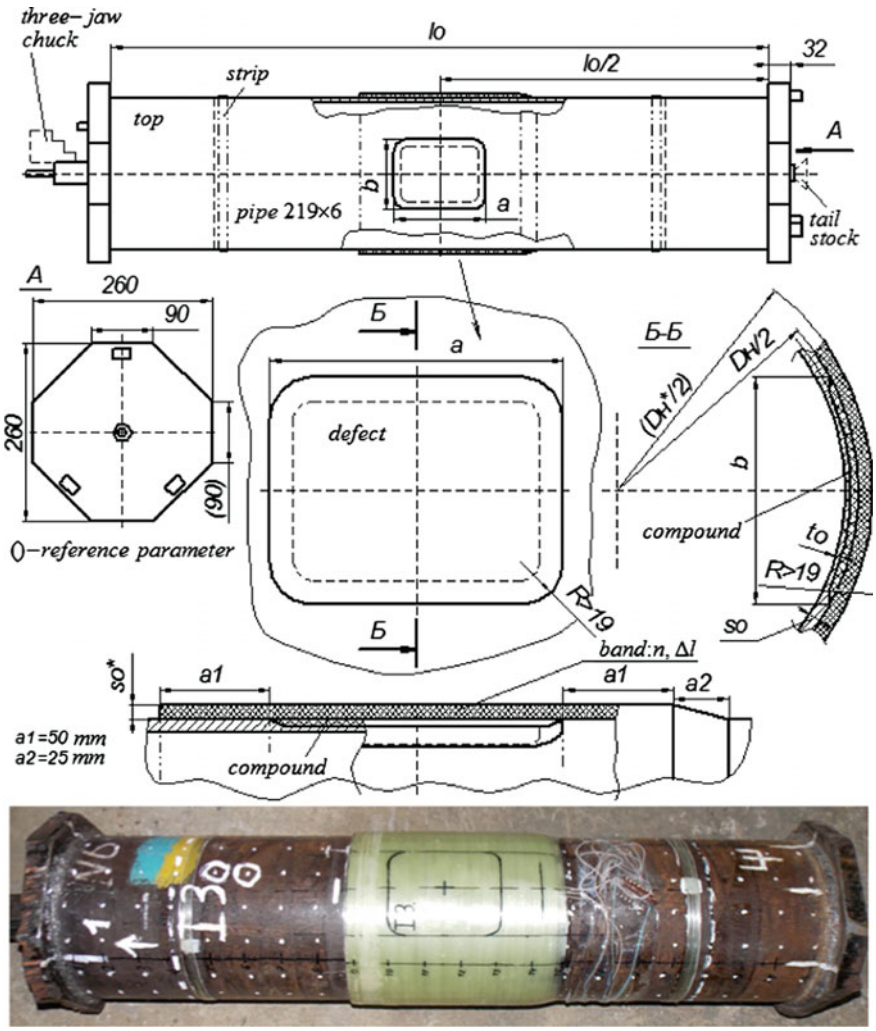

Fig. 1 Basic diagram by the example of sample I3 and its photo

deformation plasticity theory for simple loading is shown by the example of sample I4. Regardless the fact that relationship of axial and circumferential stresses in the pipe in this case is not constant, i.e., loading is not simple, nevertheless the experimental data showed the possibility of such approximation that significantly simplifies a problem [8]. With some complements, this approach can be used for the calculation of composite wrap on a pipeline damaged section.

Let us consider the main provisions of calculation. Since the ultimate deformations of the wrap are insignificant, the calculation is carried out on the initial geometry and tensile diagram. Effect of preliminary tension of the wrap is also

insignificant and it can be neglected. Making equal circumferential deformations of pipe middle surface and wrap, an equation of mutual deformation is obtained as

$$\varepsilon_t = \varepsilon_{t^*}\frac{r_*}{r} = \frac{\sigma_{t^*}}{E_*}\cdot\frac{r_*}{r} = \frac{1}{E}(\sigma_t - \mu\sigma_z) + \left(\frac{1}{E_C} - \frac{1}{E}\right)(\sigma_t - 0.5\sigma_z) \tag{1}$$

where σ_t, σ_z are the circumferential and axial stresses in the pipe; r, s are the radius of middle surface and thickness of the pipe, respectively; ε_t is the circumferential deformations of middle surface of the pipe; E, μ is the elasticity modulus and Poisson's ratio of pipe material. A star (*) shows corresponding parameters for the wrap. $E_C = \sigma_i/\varepsilon_i$ is the secant modulus determined on curve connecting stress intensity σ_i with deformation intensity ε_i (diagram of pipe material tension in circumferential direction).

Stresses in the pipe are expressed by the following equations:

$$\sigma_z = \frac{Pr}{2s}, \quad \sigma_t = \frac{r}{s}(P - P_*) \quad \text{and} \quad \sigma_t = \frac{Pr - \sigma_{t^*}s_*}{s}, \tag{2}$$

where P, P_* are the inner pressure in the pipe and the pressure between pipe and wrap.

Expression (2) are obtained from the equilibrium condition of the part of structure cut with axial plane: $\sigma_t s + \sigma_{t^*}s_* = Pr$. The radial stresses are taken equal zero.

Inserting stresses (2) into Eq. (1) provides

$$\sigma_{t^*} = \frac{\frac{Pr}{4s}\left(\frac{3E}{E_C} + 1 - 2\mu\right)}{\frac{r_*}{r}\cdot\frac{E}{E_*} + \frac{s_*}{s}\cdot\frac{E}{E_C}}, \quad P_* = P\frac{\frac{r}{4s}\left(\frac{1-2\mu}{E} + \frac{3}{E_C}\right)}{\frac{r_*}{s_*E_*} + \frac{r}{sE_C}}. \tag{3}$$

Making the secant modulus equal to the elasticity modulus, we obtain a solution for elastic pipe deformations. As it can be seen, circumferential stresses in the wrap and outer pressure on the pipe in the elastic area are directly proportional to inner pressure.

Equation (3) is solved using a method of incremental motion on ε_i, σ_i curve set by discrete values. Employing stress intensity in the pipe $\sigma_i = \sqrt{\sigma_t^2 - \sigma_t\sigma_z + \sigma_z^2}$, corresponding to it deformation intensity, and value of the secant modulus in a previous point allows determining a current value of the secant modulus. The calculation is performed up to the moment when the wrap circumferential deformations $\varepsilon_{t^*} = \sigma_{t^*}/E_*$ will not reach the limit values.

The increase of number of the wrap layers promotes for increase of value of inner pressure, at which intensity in the pipe reaches a proportionality limit and conventional yield strength, and circumferential deformations in the wrap, compared with the limiting values. Corresponding calculated dependencies for sample I4 without preliminary wrap tension are given in Fig. 2, lines P, Y and B. As it follows from the figure, the increase of the number of the wrap layers has more

significant effect on serviceability of the wrap (curve B) than on elastic deformation ability of the pipe metal (curves Y, P). It should be noted that these dependencies are not strictly linear, each following layer increases the limit pressure by a smaller value, than the previous one.

Close correspondence of experimental data (indicated by bold marks) and calculated values (curves P, Y, B) show sufficiently high accuracy of SSS prediction for selected number of the wrap layers (8).

Detailed ultrasonic thickness measurement of cylinder metallic part of the samples, including defects, was carried out before tests and after their finishing. The values of thickness were measured at the points equally distributed over the surface. Working and calibrating pressures (similar for all samples) were assigned in accordance with [9–12] taking into account the results of determination of mechanical properties of pipe material and thickness measurement.

The wire strain gauges of 10 mm base were glued on outer metallic surface of the samples (except for sample I1) in regular (distant from the effect of defect and bottoms) zone in circumferential and axial directions for the measurement of elasto-plastic deformations. The strain gauges were also set in the defect central zone and on the wraps after their assembly. Deformation was measured under load and after its rejection. Complete deformations under loading were determined considering accumulated residual deformations. All strain gauges were duplicated. The strain gauges on wraps of samples I3 and I4 were located over the strain gauges glued to pipe metal.

Measuring bases were applied in the regular part and in the defect using punching in circumferential and axial directions. They were used for determination of residual plastic deformation after the next stage of loading as well as fracture. Measurements under the wrap on samples I3 and I4 were carried out only after

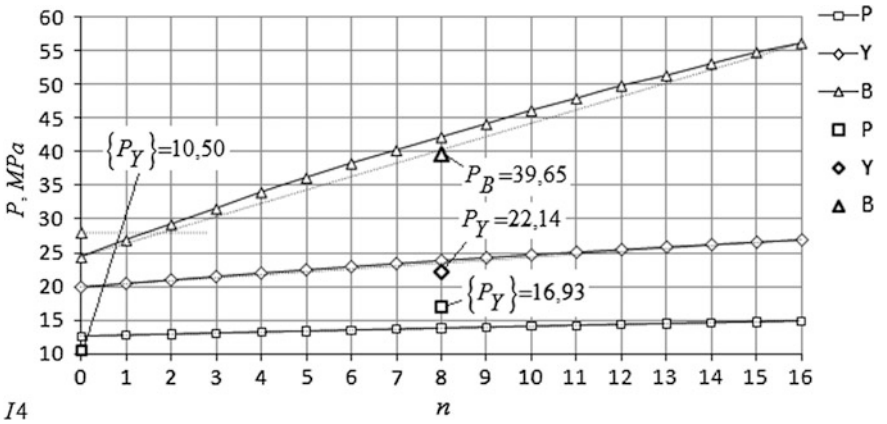

Fig. 2 Effect of the number of wrap layers on critical pressure value determined by: stress in a vessel wall, corresponding to a limit of proportionality of stress intensity (*line P*); stress in a vessel wall corresponding to conventional yield strength (*line Y*); limiting circumferential deformations in the wrap (*line B*); *bold marks* indicate the experimental data

fracture and wrap removal. Three circumferential sections were determined on each of samples I1 and I4, on which 16 measuring bases were made, for detection of the dependence of residual deformation on thickness difference. The same sections were used to control the residual deformations in axial direction. The difference between punching points on the defect surface in circumferential and axial directions was $\sim$45 mm. The distance between points was measured with the help of flexible metallic ruler by means of its mating with metal surface.

2 Peculiarities of Full-Scale Samples Testing

Tests of the samples were carried out in a hydraulic bench. Moreover, tests of samples I1 and I4 at the initial stage took place in a water jacket (WJ), which allowed determining the increase of sample volume in process of inner pressure loading as well as after its release [13]. The minimum pressure, applying of which provoked residual increase of sample volume, was taken as a yield start pressure $\{P_T\}$. Inner pressure in the sample was created using "Hofer" pump of 50 l/h efficiency. Loading was carried out in few steps. Pressure in each stage rose from zero to a set value, which exceeded the maximum pressure of the previous stage. Exposure under pressure was used after reaching the set value. At the initial stages, this time was used for taking the readings of the strain gauges, at the next stages for complete realization of plastic deformations. Digital manometer Metran 100-DI was used for pressure recording. Weight of the sample and outer perimeters of several sections of the pipe and the wrap were measured after finishing each stage (except for steps performed in the water jacket). Loading in the hydraulic bench was carried out to fracture (depressurizing) of the sample. Two receivers were embedded in a serial hydraulic circuit between the pump and test object in order to increase hydraulic system volume. This allowed reducing a pressure growth rate and provide for smoother loading. The testing water temperature was into 10–23 °C range. A diagram of sample loading, simulating pipe in as-delivered condition, is shown in Fig. 3 as an example.

Below are given the main peculiarities of sample testing.

I1: ***Pipe in as-delivered condition***. Loading was carried out in the water jacket and at plastic deformations close to the limit strains; it was performed in the hydraulic bench (HB). After full-scale sample fracture, it was used for cutting out the samples, which were subjected to uniaxial tension tests. The samples were cut in circumferential and axial directions from the zones with residual plastic deformation set on punched base measurement. The samples for hardness measurement were cut out close to previous specimens.

I2: ***Simulation of damaged section of the pipeline***. Loading was carried out in HB with simultaneous measurement of deformations with the help of strain gauges.

I3: ***Model of damaged section of the pipeline repaired using composite wrap***. After the stain gauges, mounted on the defect in circumferential direction, start

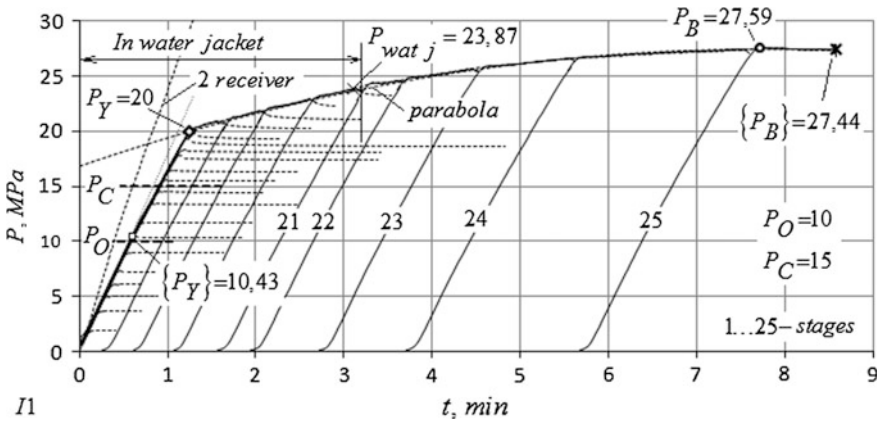

Fig. 3 Stages of loading with inner pressure to sample fracture I1: $P_{\text{wat},j}$ is the pressure to which the sample was loaded in water jacket; 2 receiver is the diagram of loading of two twin receivers without testing object; parabola is the line of approximation of diagram of sample loading in plastic area by second-degree equation with a peak in P_B point; *fine dashed lines* are the exposure at loading stages; other designations see in Table 3

registering residual deformations, a wrap was installed on the sample and pressure loading was renewed.

I4: ***Model of strengthened part of the pipeline***. Loading was carried out in the water jacket before residual volume increase. Then, the strain gauges were mounted on the pipe surface and the sample was subjected to secondary loading to a pressure $\leq \{P_T\}$ in HB. After wrap winding and setting the strain gauge on its surface the sample was ones more subjected to loading to a pressure $\leq \{P_T\}$ in HB. Then, the tests were continued in WJ. The tests in HB were finished at deformations close to the limit strains.

Manufacture and testing of the full-scale samples was carried out in the I1-I2-I4-I3 order. This sequence allows correcting the parameters of current tests, based on the test results of previous samples. For example, the wrap of sample I3 was manufactured considering the results of testing of composite material in I4 sample, behavior of non-strengthened defect of sample I2 as well as fracture pressure of sample I1, which was set as a fracture required pressure.

Figure 4 shows the equipment used for hydraulic tests.

3 Main Test Results

The results of the determination of the mechanical properties, composition of material and other main parameters of the pipes are given in Tables 1 and 2.

Table 1 gives the results of tension of the samples with minimum values of ultimate strength. It should be noted that the group of the samples cut out in

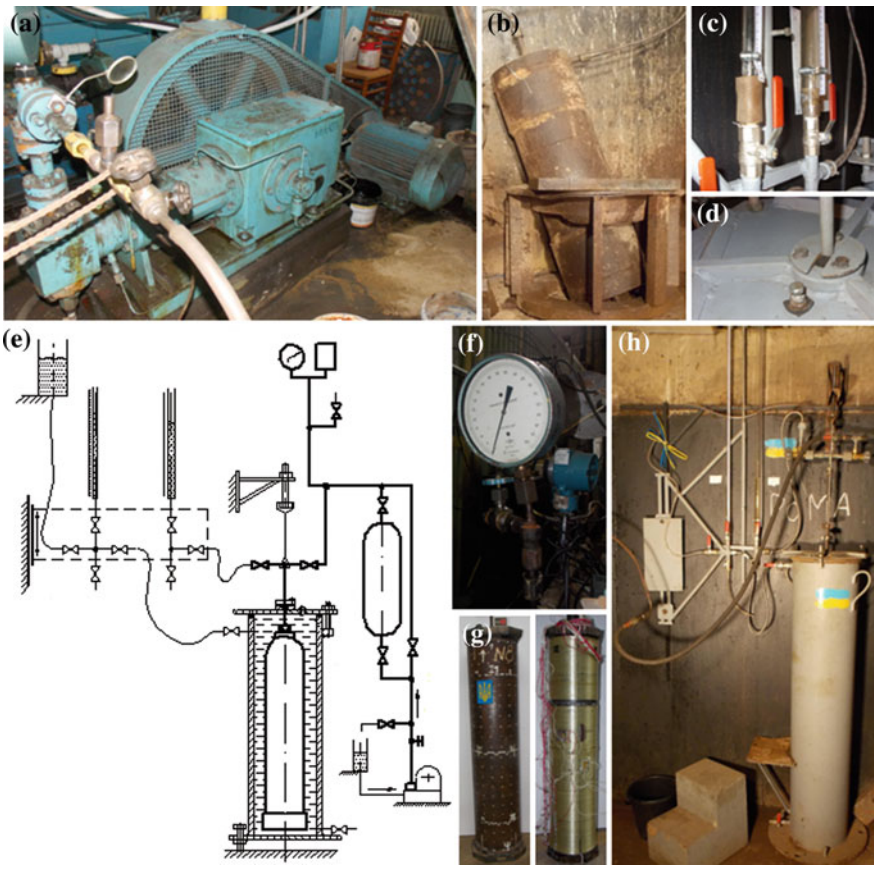

Fig. 4 Equipment for hydraulic tests of vessels (PWI): **a** "Hofer" pump; **b** receiver; **c** burette connection; **d** system of air made from "water jacket"; **e** basic diagram of test system; **f** manometer and Metran 100-DI pressure probe; **g** samples tested by inner hydraulic pressure; **h** "water jacket" installation

Table 1 Mechanical properties of pipe material

According to		σ_t (MPa)	σ_y, σ_{02} (MPa)	δ (%)
GOST 8731-74, п.1.2. B		412.00	24.00	21.0
Manufacturer's certificate		475.78	323.73	32.0
		480.69	328.64	33.0
Mechanical tests[a]	C	474.76	305.00	33.1
	A	461.40	314.00	41.0

[a]C, A are the samples cut out in circumferential and axial directions of the pipe, respectively

Table 2 Pipe material composition

According to	Weight fraction of elements (%)							
	C	Mn	Si	S	P	Cr	Ni	Cu
GOST 1050-88	0.17–0.24	0.35–0.65	0.17–0.37	<0.040	<0.035	<0.25	<0.30	<0.30
Manufacturer's certificate	0.19	0.54	0.29	0.02	0.011	0.07	0.05	0.08
Chemical analysis	0.177	0.55	0.289	0.018	0.008	0.078	0.065	0.070

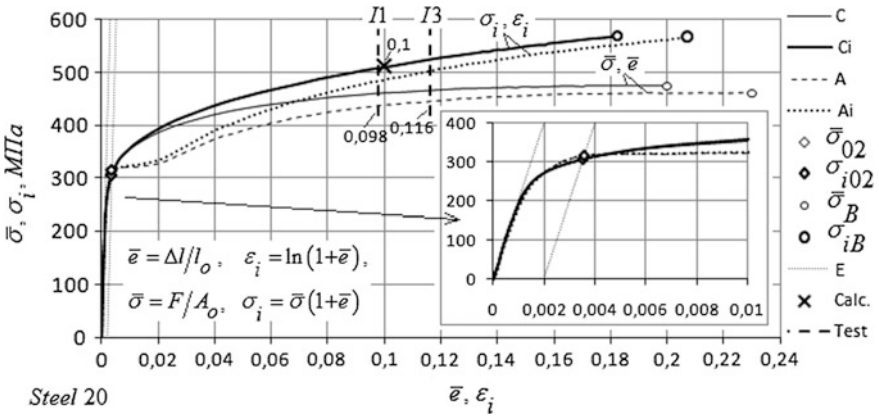

Fig. 5 Diagrams of tension $\bar{\sigma}, \bar{e}$ of samples cut out in circumferential and axial directions of pipe in initial condition, and actual deformation diagrams plotted on them: C, A are the diagrams of sample tension in circumferential and axial directions; C_i, O_i are the actual diagrams of deformation, respectively; $\bar{\sigma}_{02}, \bar{e}_B$ are the conventional stresses; $\sigma_{i02}, \sigma_{iB}$ are the actual stresses; E is the dependence of stresses on deformations in elastic area ($E = 2 \times 10^5$ MPa)

circumferential direction were subjected to complete leveling in a press by four-point bend test, the other group was leveled only in the grip places, a test portion remaining non-deformed. Obtained results showed that the values of conventional yield strength of completely leveled samples are ~5% higher, the rest of parameters are not different. The samples, cut out in axial direction, were not leveled, the places for grips the same as in circumferential samples were polished. The sides of all samples, corresponding to inner and outer pipe surface, were not mechanically treated.

Figure 5 shows conventional and actual tension diagrams to the moment of start of formation of neck of the samples cut out from the pipe at initial condition, in circumferential and axial directions. The following dependencies were used for plotting an actual diagram of deformation:

$$\varepsilon_i = \ln(1+\bar{e}), \quad \sigma_i = \bar{\sigma}(1+\bar{e}), \tag{4}$$

where ε_i and σ_i are the intensity of logarithmic deformations and actual stresses, respectively, $\bar{e}$ and $\bar{\sigma}$ are the deformations and stresses determined from conventional tension diagram. The actual deformation diagram is invariant in relation to type and sequence of loading that is also verified by the results of present investigations.

Figure 5 also indicates the calculation and experimental values of deformation intensity corresponding to limiting state of the full-scale samples I1 and I3.

The conducted investigations showed that the pipe taken for manufacture of the full-scale samples had significant thickness difference that is caused by hot-worked production technology. Wall thickness distributions before and after tests are characterized by left-side asymmetry (Fig. 6). After fracture, the average thickness is reduced by 4.3% and standard deviation due to more intensive deformation in thinner areas rises 1.5 times.

The performed statistical processing of thickness measurements (n = 352) allowed making some observations useful for practical application

(i) an average value, based on 16 measurements in a random cross-section, differs not more than 0.75% from average thickness value, determined on the results of all carried measurements; the deviation becomes <1.2% in the case of eight measurements.
(ii) cross-section of hot-worked pipe is sufficiently well described by two eccentric circumferences of different diameter.

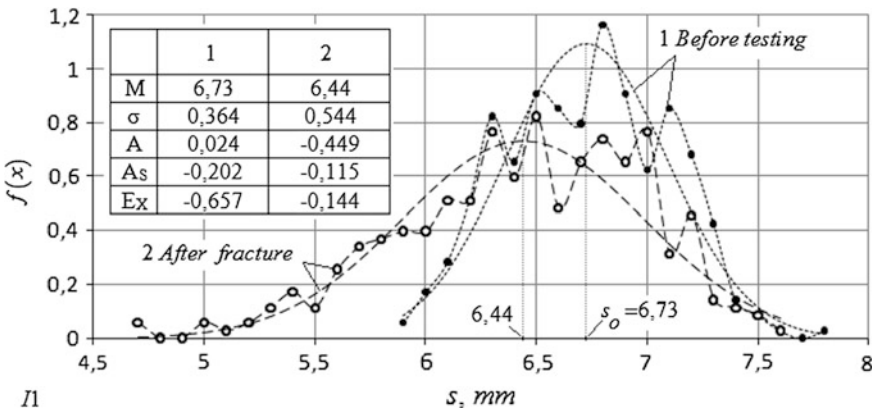

Fig. 6 Distribution of wall thickness in sample I1 before and after hydraulic tests with inner pressure to fracture: $f(x)$ density distribution; M average value; σ standard deviation; A third central moment (asymmetry); A_S asymmetry relative index; E_X fourth central moment (excess); *fine lines* show distributions under the assumption of their normality; *pointed points* correspond to thickness range 0.1 mm

Table 3 Generalized data on full-scale samples I1, I2, I3 and I4

Parameter		Unit of measurement	Sample designation			
			I1	I2	I3	I4
Hollow billet						
Outer diameter, D_O		mm	220.15	219.77	220.15	219.99
Wall thickness of hollow billet	Average, s_O	mm	6.73	6.76	6.89	6.55
	Minimum, s_{min}	mm	5.9	6.1		5.7
Internal volume, W_o		l	32.0	31.9		31.,8
Length between bottom inner surfaces, l_o		mm	953.00	953.25	954.50	956.50
ΔW_{evc}, per 1 MPa, to pressure $\{P_Y\}$; method of least squares		cm^3	5.329	–	–	5.702
Yield pressure, $\{P_Y\}$		MPa	10.43	–	–	10.50
Defect						
Wall thickness in defect	Average, t_o	mm	–	2.70	2.82	–
	Minimum, t_{min}	mm	–	2.4	2.3	–
Linear dimensions, [length (a) × width (b)]			–	133 × 102		–
Design factor of strength reduction				0.499	0.493	
Yield pressure, $\{P_Y\}$		MPa	–	5.83	5.93	–
Composite wrap						
Wrap outer diameter, D_{O^*}		mm	–	–	232.59	225.02
Number of wrap layers, n		psc	–	–	16	8
Wrap thickness, s_{0^*}		mm	–	–	6.22	2.52
Thickness of wrap layer, Δr		mm	–	–	0.389	0.315
Winding step Δl		mm/rev	–	–	2.36	2.36
ΔW_{evc}, per 1 MPa, to pressure $\{P_Y\}$; method of least squares		cm^3	–	–	–	5.024
Yield pressure, $\{P_Y\}$		MPa	–	–	16.65	16.93
Loading diagram						
Yield pressure, $\{P_Y\}$		MPa	20.00	–	19.60	22.14
Maximum pressure, P_B		MPa	27.59	13.83	29.06	39.65
Fracture pressure, $\{P_B\}$		MPa	27.44	13.83	29.03	33.87
Safety factor n_B		–	2.76	1.38	2.91	3.97
Safety reduction/increase factor, φ		–	1	0.501	1.053	1.437
Measured operating and check pressure						
Operating pressure, P_O		MPa	10			
Check pressure, P_C		MPa	15			

Note $\{P_Y\}$ is the yield pressure determined on water jacket for samples I1 and I4, and on circumferential stress gauges in the defect for samples I2 and I3; P_Y is the yield pressure determined as a culminating point of diagram of inner pressure loading; ΔW_{evc} is the elastic volume change

Fig. 7 Full-scale samples I1, I2, I3 and I4 after fracture by hydraulic inner pressure

Combined data on geometry parameters of the samples and the main results of their hydraulic testing are shown in Table 3. Figure 7 gives the photos of the samples tested to fracture. Absence of chips, peculiarities of fracture surface and fracture line trajectory indicate ductile fracture of metal of the full-scale samples [14].

References

1. GOST 1050-88. *Rolled Section, Calibrated with Special Surface Finishing from Carbon Quality Structural Steel. General Specification* (1988) (in Russian)
2. GOST 8732-78. *Hot-Rolled Seamless Steel Pipes. Assortment* (1978) (in Russian)
3. GOST 8731-74. *Hot-Rolled Seamless Steel Pipes. Specification* (1974) (in Russian)
4. API 579-1/ASME FFS-1. *Fitness for Service*
5. GOST 17139-2000. *Glass Fiber. Roving. Specification*. Minsk (2000) (in Russian)
6. TU-U 24.6-0030314547-002-2004. *Epoxy Binder of KDA-KhI Grade* (2004) (in Russian)
7. *Versatile Epoxy Glue of "Khimkontakt - Epoxy"*, TU-U 24.6-2558309112-006-2006 (2006) (in Russian)
8. I.F. Obraztsov, V.V. Vasilev, Bunakov V. A. *Optimum Armoring of Rotational Shells of Composite Materials*. Moscow, Mashinostroenie, 144 (1977) (in Russian)
9. GOST 8731-74. *Metallic Pipes. Hydraulic Pressure Testing Method* (1974) (in Russian)
10. GOST 3845-75. *Metallic Pipes. Hydraulic Pressure Test Method* (1975) (in Russian)

11. V.M. Belayev, V.M. Mironov. *Design and Calculation of Elements of Branch Equipment. P. I: Thin Wall Vessels and Apparatuses of Chemical Industry* (Tomsk Polytechnic University Press, Tomsk, 2003), p. 168 (in Russian)
12. GOST 14249-89. *Vessels and Apparatuses. Norms and Methods of Strength Calculation*
13. R.I. Dmytriienko, E.F. Garf, V.P. Chizhenko. *Technical Diagnostics and Non-destructive Testing*. **1**, 23 (2014) (in Russian)
14. ISO 9809-1:2010(E). *Gas Cylinders—Refillable Seamless Steel Gas Cylinders—Design, Construction and Testing. Part 1: Quenched and Tempered Steel Cylinders with Tensile Strength Less than 1100 MPa* (2010) (in Russian)